International Journal of Engineering & Technology, 4 (2) (2015) 381-389
www.sciencepubco.com/index.php/IJET

doi: 10.14419/ijet.v4i2.4603
Research Paper

Application of cooling, heating loads in an autonomous microgrid as a control strategy

Mostafa Vahedipour Dahraie*, Homa Rashidizadeh Kermani, Hamid Reza Najafi

Department of Electrical Engineering, Birjand University, Birjand, Iran
**Corresponding author E-mail: vahedipour_m@birjand.ac.ir*

Abstract

In this paper, a control scheme is proposed for a microgrid. In the proposed scheme, by controlling cooling, heating loads (C/H loads), balance between generation and consumption power is kept, and the frequency remains within its nominal value. Application of storage systems imposes costs, operating and maintenance problems to the microgrid owners. Moreover, the charge and discharge process of batteries causes reduction in their lives time. The dominant concept of this scheme is to control frequency without any storage. In this case, the coincidence of generation and consumption in C/H load technology is not necessary. This control system changes the consumption power of C/H loads and responses to unbalance power of microgrid, fast. Moreover, two indices are defined to assess the performance of the microgrid.

Keywords: *Microgrid; Distributed Generation; Synchronous Generator; Wind Turbine.*

1. Introduction

Microgrids are defined as systems that have at least one distributed energy resource (DER) and associated loads, which can perform in electrical distribution systems and provide better power quality to the end customers independently compared with the traditional utility [1]. Microgrids can also contribute in global emissions and energy losses. Technical challenges which pertain to their operational and control problems are immense. So the microgrid structure poses various problems such control and protection, power quality and stability issues.
In an attempt to assess transient performance and penetration level of wind turbines, reference [2] tries to present a simulation algorithm. In the aforementioned paper, a Wind Diesel Hybrid System (WDHS) is simulated and studied under different conditions. In reference [3] WDHS is modeled with variable-speed flywheel energy storage in accordance with hydrostatic transmission.
Reference [4] models WDHS in the presence of the energy storage system. In this model a Ni–MH battery based Energy Storage System tries to absorb or inject active power in order to control frequency. Different strategies are proposed to share loads properly between resources and consequently, the frequency would be kept within its standard permissible level, and the transient behavior of microgrids would improve [5-7].
Maintaining the voltage and frequency within the standard permissible level is an important requirement in microgrid design procedures. Various control approaches have been developed to maintain them in the microgrid [8-11].
Many microgrid projects focus on delivering power while other forms of energy need, such as heat, are necessary. So the combined cooling, heating and power (CCHP) are proposed [1]. A microgrid could be constructed from the most economical combination of heat and electricity. Unlike electricity, heat, usually in the form of steam or hot water, cannot be easily or economically transported long distances. So the combination of heat and electricity typically provide heat for industrial processes, on-site space heating, local district heating, for domestic hot water or sterilization in a hospital.
There are three immediately apparent potential applications of heat and electricity in microgrids [1]:

1) Space heating, domestic hot water heating and sterilization;
2) Industrial or manufacturing processes;

3) Space cooling and refrigeration through use of absorption chilling.

In this paper, C/H load scheme is used in an autonomous microgrid in order to keep balance between generation and demand. In this strategy, the microgrid frequency is kept within its allowed limitation with the fast response controller. The performance of the proposed controller strategy is studied under different conditions in a microgrid.

This paper is organized as follows: Section 2 explains the microgrid system model. In Section 3 the simulation results are presented and in part 4 a brief conclusion is reported.

2. System model

The under study system is illustrated in "Fig. 1". The system has three feeders, two DGs, loads and control system. DG1 is a synchronous generator (SG) driven by a diesel engine. The SG is equipped with a turbine-governor and automatic voltage regulator systems, connects to Bus1. DG2 is a Wind Turbine with an asynchronous generator (WTG) connects to Bus2. Furthermore, load and C/H load controller connect to Bus3. The microgrid is assumed to be operational and can meet corresponding loads in isolated mode. The single-line diagram of the system is shown in "Fig. 2."

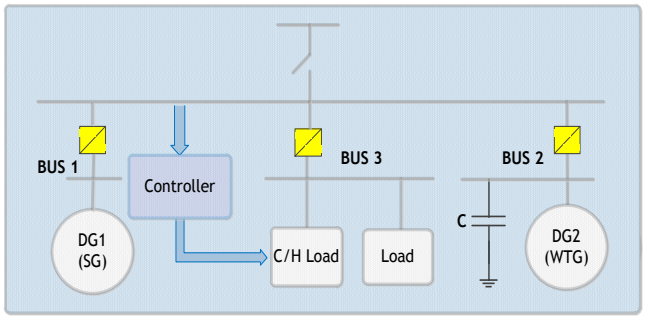

Fig. 1: The Autonomous Microgrid

2.1. System reference frame

The state-space of DGs and network are represented on their individual local reference frame. "Fig. 3" shows a Global and local rotating reference frame of the study system. A common reference frame is considered as the global reference frame and all the local parts are translated to the global reference frame using the transformation technique defined in (1) [12].

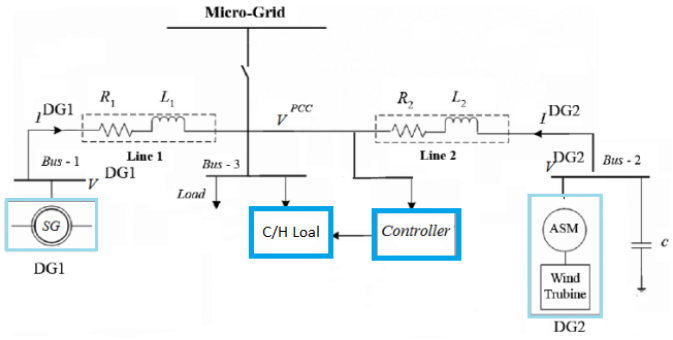

Fig. 2: The Single Line Diagram of the Microgrid.

In "Fig. 3," the axis d-q is the global reference frame based on the network rotating at the angular frequency of ω, where axis d1-q1 and d2-q2 are the reference frame of DG1 and DG2 rotating at ω_1 and ω_2, respectively. δ_n Is the angle between the reference frame of dn-qn and the global reference frame?

$$\begin{bmatrix}\Delta f_{qn}\\ \Delta f_{dn}\end{bmatrix}=\begin{bmatrix}\cos\delta_n & -\sin\delta_n\\ \sin\delta_n & \cos\delta_n\end{bmatrix}\begin{bmatrix}\Delta f_q\\ \Delta f_d\end{bmatrix}+\begin{bmatrix}-f_{dn}^{o}\\ f_{qn}^{o}\end{bmatrix}\Delta\delta_n \tag{1}$$

The voltage or current component, and o r represents presents the steady-state value.

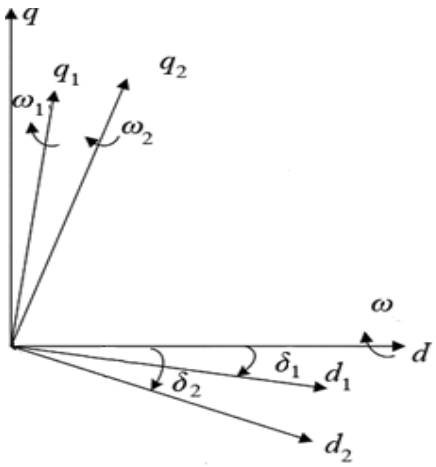

Fig. 3: Global and Local Rotating Reference Frame of the Study System

2.2. Model of DG1

DG1 consists of a prime mover such as a diesel engine, and a three-phase synchronous generator with excitation and governor control systems. The generator and the diesel engine are mechanically coupled. The turbine-governor system of SG controls the power-frequency characteristics. The electrical system of the SG modeled in d-q frame of the reference frame [13], which is identified by d–q in "Fig. 3," is given by.

$$V^{DG1} = GI^{DG1} + H\frac{d}{dt}(I^{DG1}) \tag{2}$$

Where

$$V^{DG1} = \begin{bmatrix} V_{q1} & V_{d1} & V_{k1q1} & V_{k2q1} & V_{kd1} & V_{fd1} \end{bmatrix}^T \tag{3}$$

$$I^{DG1} = \begin{bmatrix} I_{q1} & I_{d1} & I_{k1q1} & I_{k2q1} & I_{kd1} & I_{fd1} \end{bmatrix}^T \tag{4}$$

Are vectors of voltages and currents of the stator winding (d_1, q_1), damper windings (k_1q_1, k_2q_1, $k\ d_1$) and field winding (fd_1). Matrices G and H are given in [13].

The dynamic model of the rotating mechanical system of DG1 is given by.

$$J\frac{d^2}{dt^2}(\delta_1) + D\frac{d}{dt}(\delta_1) = T_m - T_e \tag{5}$$

Where J and D are the inertia and damping constants, respectively. T_m And T_e are the mechanical and the air-gap torques, respectively [13] and

$$T_e = \frac{3}{2\omega_r}(v_{q1}i_{q1} + v_{d1}i_{d1}) \tag{6}$$

The excitation and governor systems of DG1 are represented by a generic dc excitation system [14], and the IEEE governor model based on the speed-droop characteristic [15].

2.3. Model of DG2

DG2 is an environmentally-friendly power generation source which captures the kinetic energy of wind and transfers it to the electrical part through a gearbox [16]. The electrical model of DG2 in d-q frame is given by.

$$V^{DG2} = KI^{DG2} + Z\frac{d}{dt}(I^{DG2}) \tag{7}$$

Where

$$V^{DG2} = \begin{bmatrix} V_{sq2} & V_{sd2} & V_{rq2} & V_{rd2} \end{bmatrix}^T \tag{8}$$

$$I^{DG2} = \begin{bmatrix} i_{sq2} & i_{sd2} & i_{rq2} & i_{rd2} \end{bmatrix}^T \tag{9}$$

Are vectors of voltages and currents of the stator winding (d_1, q_1), s and r represent the stator and rotor windings, respectively. Matrices K and Z are given in [13].
The dynamic model of the rotating mechanical system of DG2 is given by

$$\frac{d}{\omega_b dt}(\omega_r) = \frac{1}{2H}(T_e - T) \tag{10}$$

Where ω_b and ω_r are basic and rotor angular velocity and H, T and T_e are the inertia constant, mechanical and electromagnetic torques, respectively; and

$$T_e = X_m(i_{sq2}i_{rd2} - i_{sd2}i_{rq2}) \tag{11}$$

Where X_m is the mutual reactance between rotor and stator windings [13]. The characteristic of the wind turbine is given as follows:

$$\lambda = R_c \frac{\omega_{wind}}{V_{wind}} \tag{12}$$

$$T_W = 0.2\rho\pi C_T(\lambda, \beta)V_{wind}^2 R_c^3 \tag{13}$$

Where T_W is the mechanical output torque of the wind turbine; ρ is the air density; C_T is the performance coefficient; λ is the ratio of rotor blade tip speed to wind speed; R_c is the turbine swept radius; β is the blade pitch angle; V_{wind} is the wind speed; ω_{wind} is the angular velocity of the wind turbine. The wind turbine connects with asynchronous generator through a coaxial shaft whose mechanical model can be expressed as a first-order system is given as follows:

$$\frac{dT}{dt} = \frac{1}{T_H}(T_W - T) \tag{14}$$

Where T_H is the inertia time constant?

2.4. Cooling, heating load controller

The dominant concept of this scheme is to control frequency without any storage. To reach this objective, two controllers are embedded: The local controller and the C/H load controller. The local controller is the conventional controller being in the SG is mentioned in [12]. And the C/H load is a general controller operating in power variations. During a change in power demand, the frequency varies. So it is required to use a frequency controller to maintain it within its nominal value. In order to reach this objective, some non-critical loads applied as C/H loads are embedded to track frequency fluctuations. C/H load controller consists of eight sets of three-phase resistors connected in series with GTO thyristor switches. The nominal power of each set follows a binary progression so that the load can be varied from 50kW- 100kW by steps of 1kW. The frequency is controlled by the Discrete Frequency Regulator block. This controller uses a standard three-phase Phase Locked Loop (PLL) system to measure the system frequency. The measured frequency is compared with the reference frequency (60 Hz) to obtain the frequency error. This error is integrated to obtain the phase error. The phase error is then used by a Proportional-Differential (PD) controller to produce an output signal representing the required C/H loads. This signal is converted to an 8-bit digital signal controlling switching of the eight three-phase loads. In order to minimize voltage disturbances, switching is performed at zero crossing of voltage. The performance of this controller is in this way that while encountering a frequency increase, the C/H load would be switched ON to absorb the active power to convert it in to cool or heating energy. So the frequency reduces to reach its rated value. As the frequency comes down, the switches open and the step of C/H load outage occurs.

On the other hand, in some states the frequency reduction might happen, for example, with increment of daily load or decrement of wind speed. So C/H load absorbs low power at this time.

3. Simulation

Load curve illustrates variation of load demand during a specific period. A typical load curve which can be an industrial unit or a hospital daily load curve is shown in "Fig. 4".

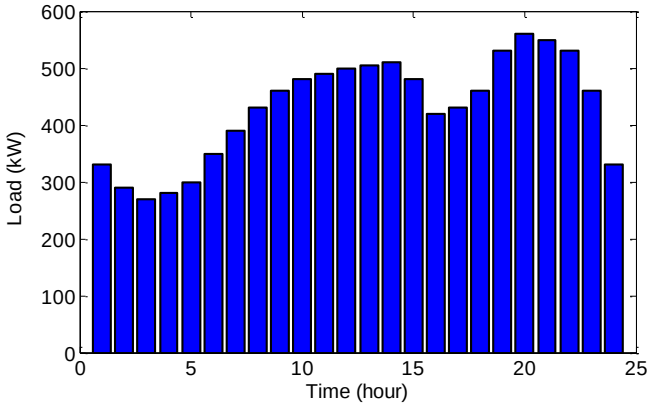

Fig. 4: Daily Load Curve of Microgrid

The steady-state output power of the under study wind turbine is illustrated in "Fig. 5". Below the cut-in wind speed, of about 4.5 m/s, the wind turbine remains shut down as the power in the wind is too low for useful energy production. Then, once operating, the power output increases following a broadly cubic relationship with wind speed until rated wind speed (10m/s) is reached. Above rated wind speed the aerodynamic rotor is arranged to limit, the mechanical power extracted from the wind and so reduce the mechanical loads on the drive train. Then, in very high wind speeds (over 16m/s), the turbine is shut down.

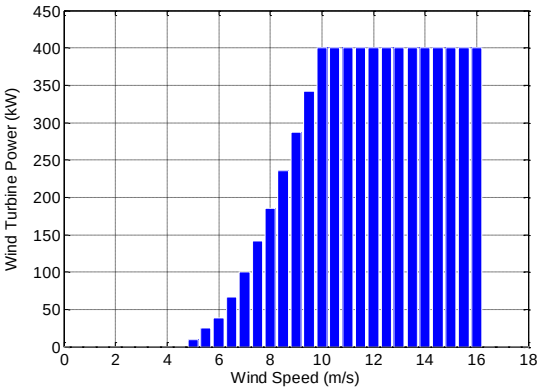

Fig. 5: Wind Turbine Power Curve

In "Fig. 6," the power consumption of load and C/H load and the generation of DG1 and DG2 during a day are depicted. It is obvious that while the wind-turbine power decreases due to the decrement of wind speed, DG1 tries to generate more power to compensate the consumption.

The wind turbine generates its nominal power in rated wind speeds. In this case, while demand is low, the microgrid frequency increases. By an increment in frequency, the C/H load tries to absorb more power to keep balance between demand and generation. So the C/H load consumption depends on power variations. While the frequency augments, its power consumption decreases and vice versa. C/H load usually heats, cooling loads, so the power variation can be applied to such loads. In this simulation, the minimum and maximum consumption of C/H load is considered to be 50kW and 100kW, respectively.

The SG comes on line whenever wind speed is low and consequently, wind turbine doesn't produce much power to supply the load. Therefore, if the wind turbine supplies both load and CCHP, the SG goes into standby mode. But when wind speed decreases, the SG power increases to supply load. As "Fig. 6" shows, SG sometimes produces its nominal power (at time =9, 12, 13, 14, 21, 22, 23, 24) so it can be used to augment the microgrid reliability. "Fig. 7". Shows the reserve power of SG during a day. Comparing "Fig. 4" and "Fig. 7" reveals that the higher the load level, the lower the SG reserve power. In this condition if the wind speed decreases, the CCHP should decline its consumption to keep frequency within its rated value.

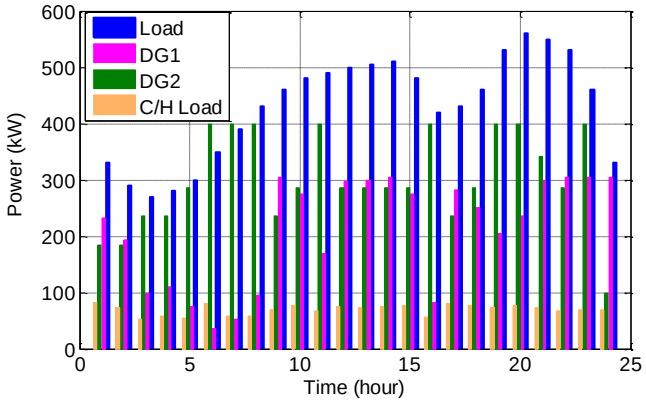

Fig. 6: Daily Generation and Demand Power of Microgrid

3.1. Index definition

Here, two indices are defined. The first one is Penetration Level index (PL index) is the ratio of wind power generation to total generation during a day. This is given as below:

$$PL\ index = \frac{wind\ \ power\ generation}{total\ \ generation} \tag{15}$$

PL index ranges between 0 and 1. With respect to stochastic nature of wind, if the average of this index during a period (a month or a year) tends to 1, the microgrid reliability decreases. So it is important to acquire this index to assess the reliability of a microgrid. Here, this factor is depicted in "Fig. 8". The average value of this index is nearly 0.6.
The other index is the ratio of C/H power to summation of CCHP. This index is given as below:

$$C/H\ \ index = \frac{C/H\ \ load}{CCHP} \tag{16}$$

C/H index ranges between 0 and 1. Whenever total generation power is consumed in C/H load, it tends to 1. Since C/H power acts in the role of a frequency controller, the higher the index, the better the performance of the microgrid. In fact, C/H power can control the frequency variations especially in high generation.
For example, it is possible to use C/H load to cool/ heat water and use it afterwards. In this case the energy can be stored in water and not wasted. The coincidence of generation and consumption in C/H load technology is not necessary.
The value of this index depends on the thermal consumption of customers. This index is calculated in the understudy microgrid and is illustrated in "Fig. 9." It is obvious that this index is between 0.1 - 0.2 during a day. It means that 10% - 20% of generation is consumed in non-electrical loads. Besides this amount of energy is used for cooling or heating, keeps the frequency within its rated value.

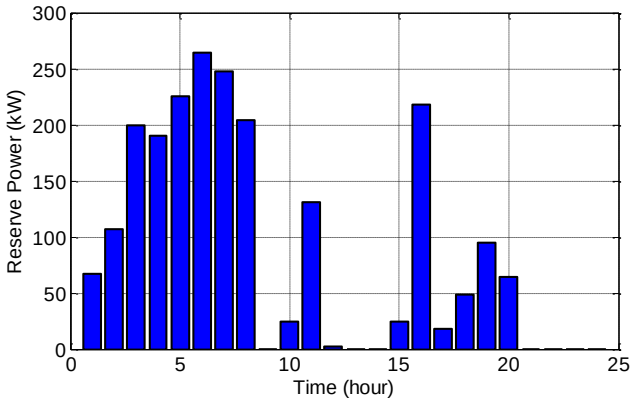

Fig. 7: Reserve Power of SG

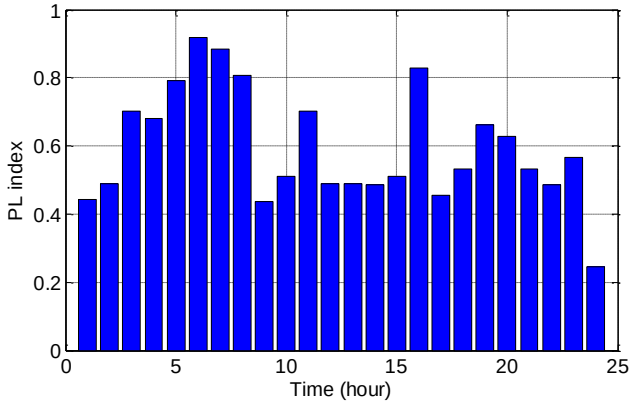

Fig. 8: PL Index in the Understudy Microgrid.

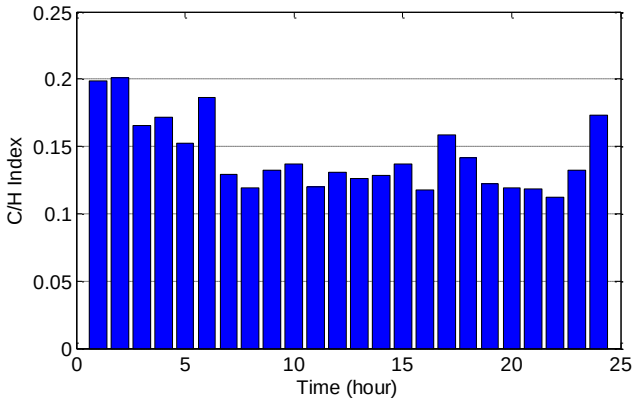

Fig. 9: C/H Index in the Understudy Microgrid

3.2. Transient study

In this section, the transient performance of the scheme is discussed.

i) Scenario A

In this scenario, the load is 460 kW+j230 kVAR and the wind speed decreases from 10 to 9 m/s, at t=10s. "Fig. 10" shows variations of active power of DGs, C/H and load in this situation. The power of WTG decreases from 400 to near 290kW and the power of SG increases. It is obvious that in high wind speed, the participation of SG is low to supply the load that causes the proposed microgrid plan to be more environmentally efficient. By decreasing the wind speed, the generated power of SG increases from 140 to 240kW. This increment compensates the low production of WTG. Increasing the production of SG, the frequency augments and as "Fig. 11" shows, it exceeds the rated value. It causes that C/H power operates quickly to control the frequency to its nominal value.

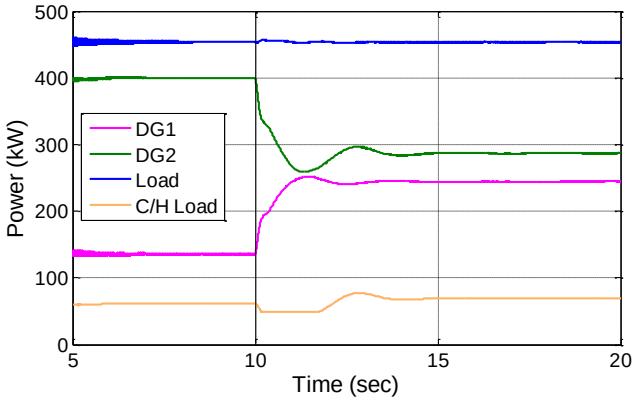

Fig. 10: Active Power of Dgs, C/H and Load (Scenario A)

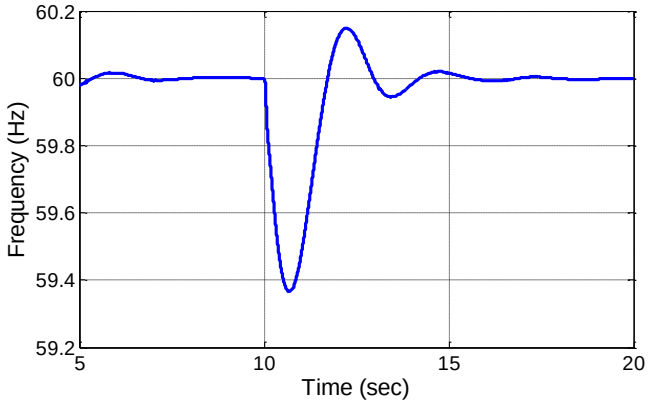

Fig. 11: Microgrid Frequency Variation (Scenario A)

ii) Scenario B

In this scenario, it is assumed that microgrid supplies three industrial units. The load of units are 200kW+j100 kVAR, 100kW+j50kVAR and 100kW+j50kVAR, respectively. In order to analyze the response of microgrid to load variations, two of units comes on-line at t=20s and t=40s. "Fig. 12" shows the active power of DGs, C/H and load. When the units come on line the frequency decreases, therefore, the generated power of SG augments to compensate the decrement of frequency. Moreover, the C/H load decreases its power to keep a frequency within its nominal value. So clearly the performance of the proposed scheme in different situations is successful.

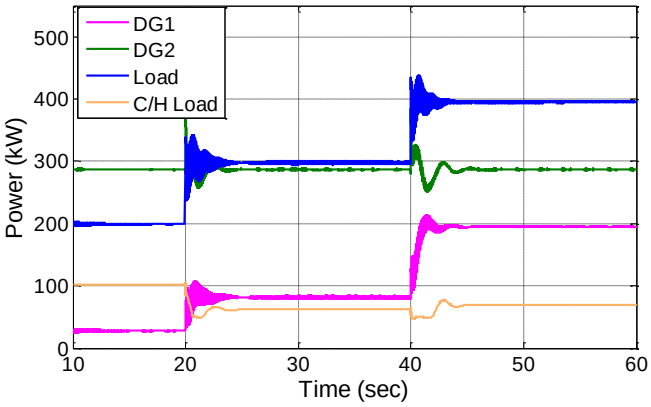

Fig. 12: Active Power of DGS, C/H and Load (Scenario B).

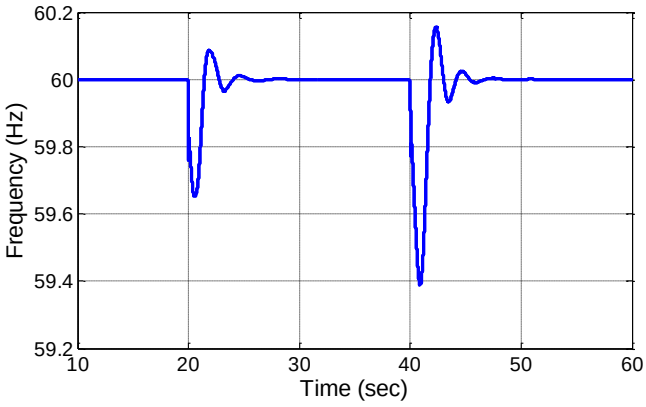

Fig. 13: Microgrid Frequency Variation (Scenario B)

4. Conclusion

In this paper, a model for the microgrid is proposed in which a C/H load scheme is used to keep balance between generation and consumption and to control frequency without storage system. As the C/H loads are insensitive, they can change their consumption. Using the C/H loads, it is possible to convert electricity to other kinds of loads (such as thermal energy) and to store it.

Moreover, the results show that the suggested scheme performs successfully and is stable due to the variation of wind speed and load demand. In order to assess the performance of the microgrid, two indices are defined.

References

[1] Kroposki, B., Lasseter, R., Ise, T., Morozumi, S., Papatlianassiou, S., Hatziargyriou, N., 2008. Making microgrids work. IEEE Power Energy Mag., 6(3):40-53. http://dx.doi.org/10.1109/MPE.2008.918718.

[2] G. S. Stavrakakis, and G. N. Kariniotakis, "A general simulation algorithm of the accurate assessement of isolated diesel-wind turbine systems interaction, Part I: A generatl multi-machine power system model" IEEE, Transactions on Energy Conversion, Vol. 10, No. 3, September 1995, pp 577 – 583. http://dx.doi.org/10.1109/60.464885.

[3] A. Tomilson, J. Quaicoe, R. Gosine, M. Hinchey, N. Bose "Modelling an autonomous wind diesel system using Simulink" ,IEEE, , Canadian Conference on Electrical and Computer Engineering ,1997, vol. 1, Page(s): 35 – 38. http://dx.doi.org/10.1109/ccece.1997.614783.

[4] R. Sebastián, R. Pe˜na Alzola "Simulation of an isolated Wind Diesel System with battery energy storage", Electric Power Systems Research 81 (2011) 677–686. http://dx.doi.org/10.1016/j.epsr.2010.10.033.

[5] Ritwik Majumder, Arindam Ghosh, Gerard Ledwich, and Firuz Zare, "Control of Parallel Converters for Load Sharing with Seamless Transfer between Grid Connected and Islanded Modes".

[6] Ali Bidram, Ali Davoudi, "Hierarchical Structure of Microgrids Control System" IEEE Transactions on Smart Grid April 09, 2012. http://dx.doi.org/10.1109/TSG.2012.2197425.

[7] Diyun Wu, K. T. Chau, Senior Member, IEEE, Chunhua Liu, Member, IEEE, Shuang Gao, and Fuhua Li"Transient Stability Analysis of SMES for Smart Grid With Vehicle-to-Grid Operation" IEEE Transactions on Applied Superconductivity, vol. 22, NO. 3, June 2012.

[8] K. T. Tan, X.Y. Peng, P. L. So, Y. C. Chu, and M. Z. Q. hen,"Centralized Control for Parallel Operation of Distributed Generation Inverters in Microgrids" IEEE Transactions on Smart Grid, 2012.

[9] K. De Brabandere, B. Bolsens, J. Van den Keybus, A. Woyte, and J. Driesen, "A voltage and frequency droop control method for parallel inverters," IEEE Trans. Power Electron., vol. 22, no. 4, pp. 1107–1115, Jul. 2007. http://dx.doi.org/10.1109/TPEL.2007.900456.

[10] J. M. Guerrero, J. Matas, L. G. Vicu-a, M. Castilla, and J. Miret, "Decentralized control for parallel operation of distributed generation inverters using resistive output impedance," IEEE Trans. Ind. Electron., vol. 54, no. 2, pp. 994–1004, Apr. 2007. http://dx.doi.org/10.1109/TIE.2007.892621.

[11] J. A. P. Lopes, C. L. Moreira, and A. G.Madureira, "Defining control strategies for microgrids islanded operation," IEEE Trans. Power Syst., vol. 21, no. 2, pp. 916–924, May 2006. http://dx.doi.org/10.1109/TPWRS.2006.873018.

[12] F. Katiraei, M.R. Iravani, and P.W. Lehn, "Small-signal dynamic model of a micro-grid including conventional and electronically interfaced distributed resources", IET Gener. Transm. Distrib, vol. 1, no. 3, pp. 369-378, May 2007. http://dx.doi.org/10.1049/iet-gtd:20045207.

[13] Krause, P.C.: 'Analysis of electric machinery and drive systems' (IEEE Press, 2002). http://dx.doi.org/10.1109/9780470544167.

[14] IEEE WG: 'IEEE recommended practice for excitation system models for power system stability studies'. IEEE STD 421.5-1992.

[15] Working Group on Prime Mover and Energy Supply Models for System Dynamic Performance Studies: 'Dynamic models for fossil fueled steam units on power system studies', IEEE Trans. Power Sys., 1991, 6, (2), pp. 753–761. http://dx.doi.org/10.1109/59.76722.

[16] S. K. Salman and A. Teo, "Windmill modeling consideration and factors infuluencing the stability of a grid-connected wind power-based embedded generator," IEEE Trans. Power Syst., vol. 18, no. 2, pp. 793– 802, May 2003. http://dx.doi.org/10.1109/TPWRS.2003.811180.